

<i>Cryst. Res. Technol.</i>	34	1999	7	859–866
-----------------------------	-----------	------	---	---------

N. G. KAKAZEY, L. A. KLOCKOV, I. I. TIMOFEEVA, T. V. SRECKOVIC¹, B. A. MARINKOVIC¹, M. M. RISTIC²

Institute for the Problems of Material Science of the National Academy of Science of the Ukraine

¹Center for Multidisciplinary Studies University of Belgrade, Joint Laboratory for Advanced Materials of SASA

²Serbian Academy of Sciences and Arts, Joint Laboratory for Advanced Materials of SASA

Evolution of the Defect Structure of Zinc-Oxide as a Consequence of Tribophysical Activation

Zinc-oxide powder was tribophysically activated in a high-energy vibro mill in a continual regime in air for 3, 30 and 300 minutes with the purpose of modifying the powders physico-chemical properties. By analyzing of data obtained by X-ray powder diffraction, electron diffraction and transmission electron microscopy, the values of distances between corresponding crystallographic planes, average domain sizes of coherent scattering, i.e. crystallites, width of diffraction lines due to the existence of microstrains, and microstrain values, minimal dislocation densities, dislocation density due to microstrain and real dislocation density, and also average distances between dislocations were determined. The dependence of these values on the activation time was established, which enabled analysis of the evolution of the defect structure of zinc-oxide powders during tribophysical activation by grinding in the described regime.

Keywords: ceramics, defects, deformation and fracture, macro defects, microstructure, X-ray techniques

1. Introduction

Due to its specific properties, zinc-oxide is greatly used for the production of materials and components for different applications (HEILAND et al.; KUZMINA et al.; BROWN). Thus, investigations of possible modifications of its properties are of both scientific and practical interest (BROWN; HIRSCHWALD et al.). Changes in properties as the consequence of tribophysical activation (TA), which is used most often in powder obtaining technologies, deserve special attention (HEINICKE). A complex analysis of activated powders is necessary, due to the great number of parameters which characterize a disperse system and multiple character of changes in the treated system material-mill-working atmosphere. In this paper, results of the analysis of the evolution of the microstructure of zinc-oxide powders tribophysically activated by grinding in a high-energy vibro mill are given. This analysis is based on data obtained using the X-ray powder diffraction (XRPD) method, electron diffraction and transmission electron microscopy (TEM).

2. Experimental procedure

A zinc-oxide powder (p. a. - Kemika - Zagreb) was used for experimental work. Its specific surface was $S_p \approx 3.6\text{m}^2/\text{g}$. The powder was tribophysically activated by grinding in a high-energy vibro mill with steel rings (CUP Mill Typ MN 954/3 KHD HUMBOLDT WEDAG AG) in air (steel vessel volume was 500cm^3 , and quantity of grinding powders was 200g; activation time $\tau = 3, 30$ and 300min), in a continual regime. X-ray diffraction lines were obtained on a X-ray powder diffractometer with $\text{Cu K}_{\alpha 1, \alpha 2}$ radiation (DRON-3). X-ray

diffraction data was used for determining the change in distances between certain crystallographic planes d (300) and (006), average domain sizes of coherent scattering D (DCS), microstrains ϵ , minimal dislocation density ρ_D , dislocation density due to microstrain ρ_ϵ , real dislocation density ρ_R , and average distance between dislocations h . A transmission electron microscope (TEM JEM-100) was also used for obtaining electron microphotographs and electron diffraction patterns (using a diaphragm whose openings had a diameter of $0.5\mu\text{m}$) for better characterization of powder particles.

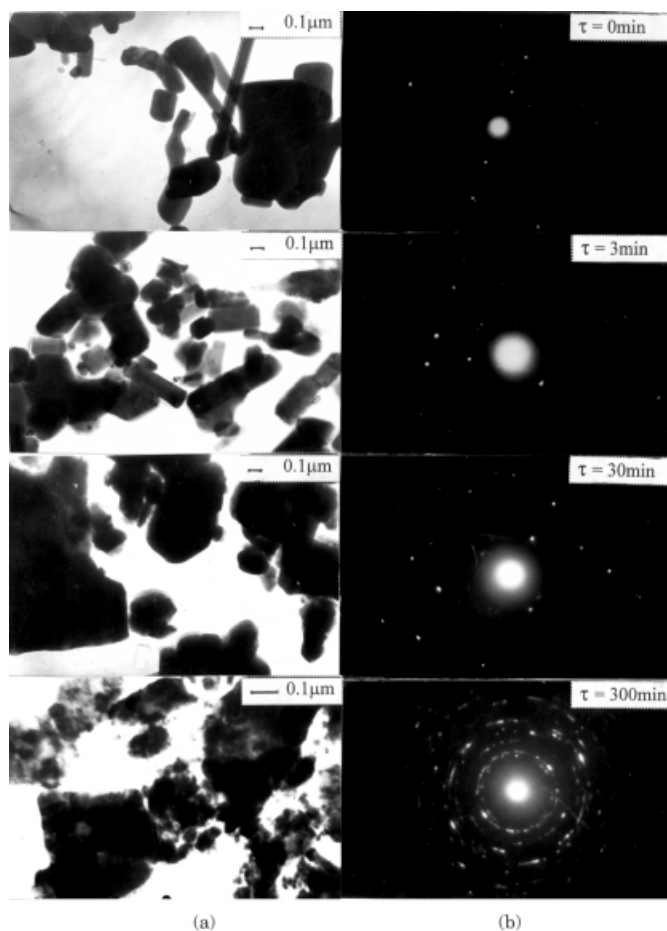


Fig. 1: Electron microphotographs (a) and electron diffraction patterns (b) of zinc-oxide powders at different stages of tribophysical activation.

3. Results and discussion

Obtained TEM microphotographs show that particles of the starting, non-activated zinc-oxide powder are characterized by shape anisotropy, from equal-axis to needle-like, with rectangular cross-sections and clearly expressed boundaries. Needle-like particles on average have a smaller cross-section, i.e. diameter of $0.1\text{--}0.2\mu\text{m}$ and length $0.4\mu\text{m}$, though in some cases it is $2\mu\text{m}$. Structures formed by agglomeration of two or more particles were also noticed. On Fig. 1a electron microphotographs of typical particles of the starting and activated powders are given, while Fig. 1 b shows electron diffraction patterns, which in the

case of non-activated powder indicates its mono-crystallinity. According to data given in (HEILAND et al.) the growth axis of such crystallites is usually parallel to the *c* axis, so in accordance with the facts stated above, the starting non-activated zinc-oxide powder can be observed on average as a assemblage of approximately similar monocrystalline particles with dimensions: 0.2μm in diameter and 0.4μm in length.

The constant value of the integral intensity of diffraction lines, enabled by the high counting statistics, permits the use of the width of diffraction lines (*B*), obtained using the approximation method (GORELIK et al.), in determining average values of the crystallite sizes D_{100} , D_{001} , i.e. microstrains ϵ_{100} and ϵ_{001} .

Having in mind, that the investigated zinc-oxide has a hexagonal crystal structure and that TEM analysis established the anisotropy of particle forms, the characteristic microstructure parameters were determined in two crystallographic directions: in the direction [100] (direction lying in the base plane) and the perpendicular direction [001]. In this sense, changes in the width of diffraction lines originating from planes (100), (300) and (002), (006) were analyzed. A non-activated zinc-oxide powder for which the K_{α_1, α_2} doublets were well separated, for the above mentioned reflections, was used as a standard. The values of full width at a half maximum of diffraction lines of the standard (b_0), i.e. instrumental diffraction line widths, were corrected in accordance with results obtained for average values of monocrystal particle sizes from microphotographs obtained using TEM and they were defined as DCS dimensions, i.e. crystallites: $D_{100} = 0.2\mu\text{m}$ and $D_{001} = 0.4\mu\text{m}$. In Table 1 values of distances between crystallographic planes *d*, average sizes of domains of coherent scattering *D*, width of diffraction lines due to the existence of microstrains ξ and microstrains *e* calculated using the above defined method are given.

τ (min)	crystall. direction	hkl	$d \cdot 10^{-8}$ (cm)	<i>D</i> (μm)	$\xi \cdot 10^{-3}$	$\epsilon \cdot 10^{-3}$
0	[100]	100	0.938(6)	0.2	0.51	0.18
		300				
	[001]	002	0.867(2)	0.4	0.46	0.17
		006				
3	[100]	100	0.938(5)	0.179	0.75	0.22
		300				
	[001]	002	0.867(4)	0.347	0.53	0.18
		006				
30	[100]	100	0.937(9)	0.098	1.25	0.28
		300				
	[001]	002	0.867(6)	0.152	0.83	0.23
		006				
300	[100]	100	0.937(2)	0.036	3.64	0.48
		300				
	[001]	002	0.867(9)	0.048	2.32	0.38
		006				

Table 1. Values of distances between corresponding crystallographic planes *d*, average sizes of domains of coherent scattering *D*, width of diffraction lines due to the existence of microstrains ξ , and microstrains *e*.

The Williams-Smallman method (WILLIAMSON et al.) and values obtained for *D* and *e* were used for calculating dislocation density:

$$\rho_D = 3n / D^2 \quad (1)$$

where *n* is the number of dislocations per the DCS face. In this estimation it was assumed

that $n = 1$, i.e. the minimal dislocation density was calculated, which corresponds to the value of the coefficient of dislocation interactions of $F = 1$ in the following expression for dislocation density:

$$\rho_{\xi} = k \cdot \xi^2 / (F \cdot b^2) \quad (2)$$

where k is a coefficient which depends on mechanical properties of the crystal, its microstructure, and also on the geometry (its values are between 2 and 25, in this case $k = 15$), and b is the Burgers vector, which is equal to the smallest interatomic distance ($b = 0.197\text{nm}$). Based on the Williams-Smallman analysis of ρ_D and ρ_{ξ} values, Table 2, it can be concluded that $n = F$, which implies the process of dislocation networking, so the real dislocation density can be determined using the expression:

$$\rho_R = (\rho_D \cdot \rho_{\xi})^{1/2}. \quad (3)$$

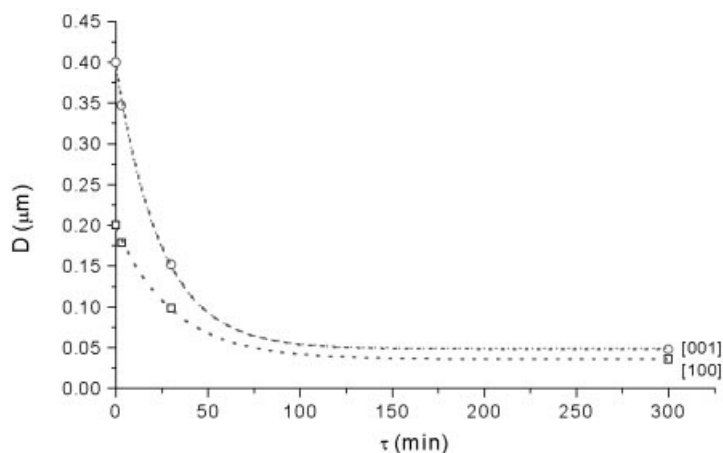
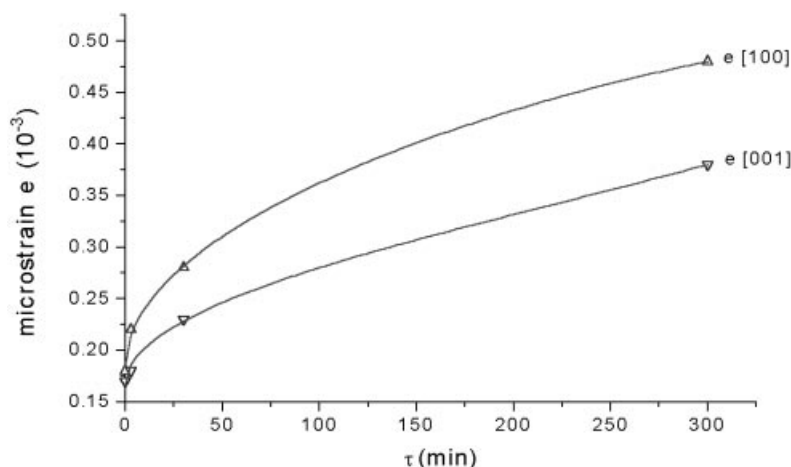


Fig. 2: Change of average crystallite sizes with the activation time.

τ (min)	crystall. direction	hkl	$\rho_D \cdot 10^{10}$ (cm^{-2})	$\rho_{\xi} \cdot 10^{10}$ (cm^{-2})	$\rho_R \cdot 10^{10}$ (cm^{-2})	$h \cdot 10^{-8}$ (cm)
0	[100]	100				
		300	0.8	1.0	0.9	1667
		002				
	[001]	006	0.2	0.8	0.4	1875
		100				
		300	0.9	2.2	1.4	1197
3	[100]	002				
		006	0.3	1.1	0.6	1441
		100				
30	[100]	300	3.1	6.0	4.3	712
		002				
		006	1.3	2.7	1.9	1039
300	[100]	100				
		300	23.1	51.2	34.4	242
		002				
	[001]	006	13.0	20.8	16.4	381

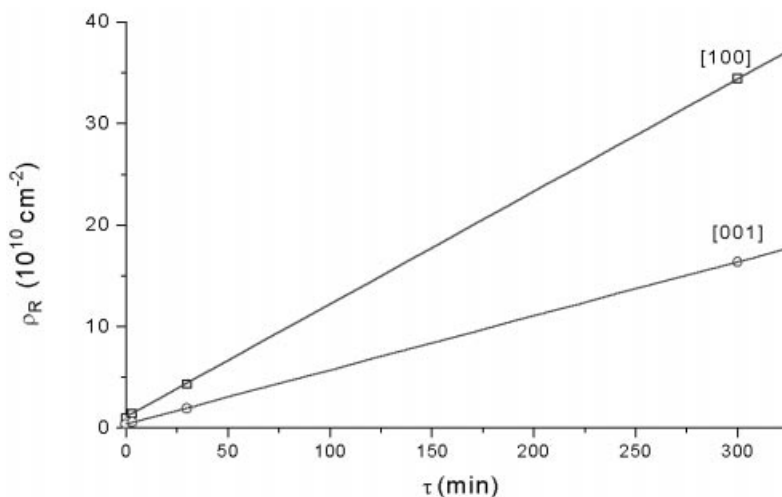
Table 2. Values of minimal dislocation densities ρ_D , dislocation density due to microstrain ρ_{ξ} and real dislocation density ρ_R , and average distances between dislocations h

Fig. 3: Change of microstrains with the activation time.



The graphical presentation of obtained results (Figs. 2 and 3) shows reduction of D_{100} and D_{001} values and increase of microstrain e with the increase of activation time, which is accompanied by a linear growth of the real dislocation density ρ_R (Fig. 4). It can be seen that the process of breaking-up of starting monocrystal particles, leading to the decrease of D values, is most intensive at the beginning of TA and is almost over after 100min of activation. Further activation is accompanied by an increase of microstrain, i.e. dislocation density with a minor reduction of crystallite dimensions. Practically equivalent microstrain values for both crystallographic directions of non-activated zinc-oxide in the stated time of ≈ 100 min were completely differentiated and further TA generally maintains the attained difference. More intensive reduction of DCS along c crystallographic direction can be explained by weaker chemical bond along this direction.

Fig. 4: Change of real dislocation density with the activation time.



Observations of the D_{100} / D_{001} ratio, which characterizes the form change of DCS, show that this ratio increases from 0.5 ($\tau = 0-30$ min) to 0.75 ($\tau = 300$ min). Having this in mind, and also electron microphotographs on Fig. 1 a, an increase of the sphericity of particles can be

indicated. In accordance with this, results obtained by electron diffraction also indicate change of the microstructure of particles of the starting zinc-oxide powder, from monocrystal to polycrystal, with the increase of TA. This effect is more pronounced with, the longer activation time and a ring-like structure of the electron diffraction pattern, characteristic for polycrystal particles, can be clearly seen for $\tau = 300\text{min}$ (Fig. 1b).

Analysis of results given in Table 2 also clearly shows the tendency of a small reduction of the interplane distance between planes (300) and increase of the interplane distance between planes (006), which indicates reduction of the lattice parameter a and increase of the lattice parameter c . Results obtained by extensive measurements of crystal lattice (KAKAZEY et al.) confirm this fact.

Decrease of the unit cell parameter a and increase of the parameter c with the increase of activation time τ is due to the formation of vacancy centers in the zinc-oxide lattice. According to EPR investigations of TA zinc-oxide powder (KAKAZEY et al., 1997) the following centers appear: a) the complex zinc vacancy - interstitial zinc atom; b) zinc vacancy (interstitial zinc atom localized at distances higher than a third of the coordination sphere); c) divacancy zinc complex, localized in one plane (001); d) oxygen vacancy. The formation of such centers in the wurcrite structure of zinc-oxide can be explained by displacement of Zn^{2+} ions (O^{2-}) from the metal sublattice (oxygen), which leads to the reduction of interatomic distances, i.e. reduction of parameter a , and the increase space between layers, which corresponds with the increase of parameter c .

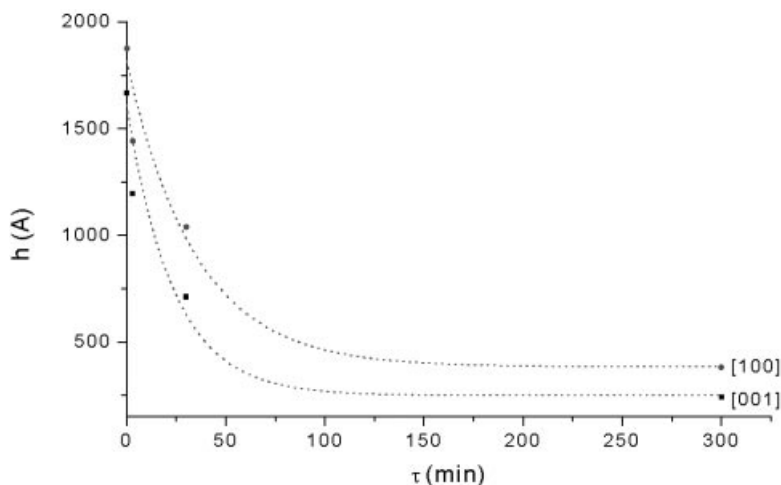


Fig. 5: Change of average distances between dislocations with activation time

DCS boundaries, formed during mechanical treatment of large crystals, are determined by the inhomogenous character of the localization of the admixture and other defects (dislocations and vacancies) in starting powders at the macro level (KAKAZEY, 1991). The existence of their complex localization structure in real powders, with a certain space periodicity can be assumed due to the existence of a great number of defect states. Triobophysical activation leads to gradual activation of this complex defect structure by further accumulation and generation of dislocations and vacancies. Having in mind all stated above, DCS evolution in activated zinc-oxide powders can be defined by the D_{100}/m and D_{001}/n ratios, where m and n are integers. Analysis of data given in Table 1 shows that $m \approx 2$ and $n \approx 3$ for powders activated for 30min, while these values are $m \approx 6$ and $n \approx 9$ for powders activated for 300min. Based on obtained values, it can be assumed that evolution of the DCS

structure in particles during tribophysical activation of zinc-oxide powders has a discrete character. It also can be concluded that DCS boundaries determine the dislocation network in starting, non-activated, powder particles. With the increase of the activation time the distances between dislocations h decrease and the level of interactions increases (Fig. 5.), which is the consequence of the increase of dislocation concentrations on the DCS surface ($n > 1$) and/or formation of dislocations with higher values of the Burgers vector \mathbf{b} . Based on this analysis, an idealized scheme of DCS structure evolution in zinc-oxide powders during tribophysical activation by grinding can be proposed (Fig. 6.).

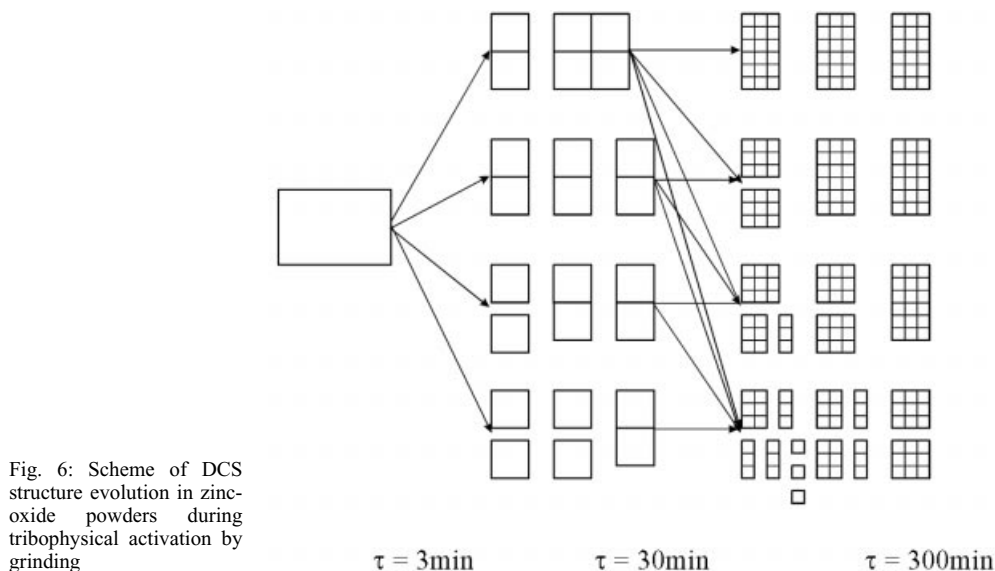


Fig. 6: Scheme of DCS structure evolution in zinc-oxide powders during tribophysical activation by grinding

Having in mind the presence of particles with different sizes and forms in the starting zinc-oxide powder, the proposed scheme of DCS structure evolution during TA grinding is approximate, though results obtained using this scheme can be used when analyzing changes of DCS dimensions during sintering such powders.

4. Conclusions

Results obtained from XPRD, electron diffraction and TEM analyses enabled the determination of characteristic microstructural parameters and establishment of the dependence of their change on the time of mechanical activation. Evolution of the defect structure of zinc-oxide powders during mechanical activation by grinding was schematically presented as DCS, i.e. crystallite evolution of the starting non-activated zinc-oxide powder.

Acknowledgment

This work was done as part of the cooperation program between SASA and IPM NANU, i.e. as part of projects "Prognosis of material properties from the viewpoint of the synthesis-structure-properties triad" and "Investigations of consolidation processes" financed by the SASA and the Ministry for Science and Technology of Serbia. The authors would also like to thank V. M. Melnikova for cooperation in the field of electron microscopic analysis.

References

- BROWN, E. H.: Zinc oxide: properties and applications, New York, Pergamon Press, 1976, 112
- GORELIK, S. S., RASTORGUEV, L. N.: Rentgenograficheskiy i elektronograficheskiy analiz metalov, Moskva, Gostehizdat, 1963 (in Russian)
- HEILAND, G., MOLLARO, E., STOCKMANN, F.: Electronic processes in zinc oxide, Solid State Phys. ed. F. Seitz and N.Y. Turnbull, London, Acad. Press., **8** 1959, 191-323
- HEINICKE, G.: Tribochemistry, Akademie-Verlag, Berlin, 1984
- HIRSCHWALD, W., P. BONASEWICZ, P., ERNST, L. et al.: Curr. Top. Mater. Sci., **7** (1981) 143-483
- KAKAZEY, N. G.: Evolution of the Defect Structure in Microcrystalline System subjected to Mechanical and Thermal Actions (by EPR Studies), D.Sc. Dissertation Abstract, Riga, (1991), (in Russian)
- KAKAZEY, N. G., SRECKOVIC, T., RISTIC, M. M.: J. Mat. Sci., **32** (1997) 4619-4622
- KAKAZEY, N. G., SRECKOVIC, T., TIMOFEEVA, I. I.: (unpublished data)
- KUZMINA, I. P. and NIKITENKO, V. A.: Zinc Oxide, the obtain and optical properties, Nauka, Moskva, 1984, (in Russian)
- WILLIAMSON, G. K., SMALLMAN, R. E.: Phyllos Mag., **1** (1956) 34

(Received May 6, 1998; Accepted August 11, 1998)

Authors' addresses:

N. G. KAKAZEY, L. A. KLOCKOV, I. I. TIMOFEEVA,
Institute for the Problems of Material Science
of the National Academy of Science of the Ukraine
e-mail: dep8@ipms.kiev.ua

TATJANA V. SRECKOVIC*, BOJAN A. MARINKOVIC
Center for Multidisciplinary Studies University of Belgrade,
Joint Laboratory for Advanced Materials of SASA,
11000 Belgrade, Kneza Višeslava 1A
Yugoslavia
e-mail: tatjanas@afrodita.rcub.bg.ac.yu
e-mail: bojan@rdc.puc-rio.br

Academician MOMCILO M. RISTIC
Serbian Academy of Sciences and Arts,
Joint Laboratory for Advanced Materials of SASA
11000 Belgrade, Knez Mihailova 35
Yugoslavia

*corresponding author